



Full Length Article



Cetuximab-conjugated andrographolide loaded chitosan-pectin composite nanoparticles for colorectal cancer

Janani Balakarthykeyan ^{a,1}, Vijayakumar Mayakrishnan ^{b,1}, Priya Kannappan ^{a,*}, Sameer Al-Ghamdi ^c, Naif Abdurhman Alrudian ^c, Mohammed Saad Alqahtani ^d, Mahmoud H. El-Bidawy ^{e,f}, Khalid Albasheer ^g, Sahar Gamil ^{e,h}, Nesreen Alsanousi ^e, Thiyagarajan Ramesh ^{e,*}

^a Department of Biochemistry, PSG College of Arts and Science (Autonomous), Affiliated to Bharathiar University, Coimbatore 641014, Tamil Nadu, India

^b Research Institute of Human Ecology, Yeungnam University, Gyeongsan 38541, Gyeongbuk, Republic of Korea

^c Department of Family and Community Medicine, College of Medicine, Prince Sattam Bin Abdulaziz University, Al-Kharj 11942, Saudi Arabia

^d Department of Internal Medicine, College of Medicine, Prince Sattam Bin Abdulaziz University, Al-Kharj 11942, Saudi Arabia

^e Department of Basic Medical Sciences, College of Medicine, Prince Sattam Bin Abdulaziz University, Al-Kharj 11942, Saudi Arabia

^f Department of Physiology, Faculty of Medicine, Cairo University, Cairo, Egypt

^g Department of Obstetrics and Gynaecology, College of Medicine, Prince Sattam Bin Abdulaziz University, Al-Kharj 11942, Saudi Arabia

^h Department of Biochemistry, Faculty of Medicine, University of Khartoum, Khartoum 11111, Sudan

ARTICLE INFO

Keywords:

Colorectal cancer
Nanocarrier
DMH
Andrographolide
5-Fluorouracil
Liver

ABSTRACT

The target specificity of drug-loaded nanoparticles can be increased by coating them with ligands that can bind to the target receptors overexpressed on the surface of cancer cells. The purpose of the current study was to examine the potential therapeutic importance of cetuximab-conjugated chitosan-pectin composite nanoparticles as novel nanocarriers for targeted delivery of andrographolide for colon cancer therapy against 1,2-dimethylhydrazine (DMH) in mice. The animals were divided into six groups: control, DMH, andro-treated group, unconjugated nanoparticle-treated group (Ch-Pec-Andro-NPs), conjugated nanoparticle-treated group (Cet-Ch-Pec-Andro-NPs), and 5-Fluorouracil-treated group (5-FU). The results from the study showed that the abnormal levels of most of the haematological, liver, and kidney tissue function markers, lipid profile, aberrant crypt foci (ACF), and colorectal markers induced by DMH were observed to be ameliorated in the treatment groups in increasing order of activity, i.e., Andro, Ch-Pec-Andro-NPs, and Cet-Ch-Pec-Andro-NPs. Despite the fact that the same amount of andrographolide was used in each treatment group, the improved therapeutic activity of Cet-Ch-Pec-Andro-NPs was attributed to the targeted delivery of andrographolide to the cancer site, which was facilitated by an anti-EGFR antibody decorated on its surface.

1. Introduction

One of the most prevalent cancers in the world, colorectal cancer (CRC) is estimated to have 1,931,590 new cases annually by the year 2020, leading to significant patient comorbidities and high healthcare costs (Sung et al., 2021). Current research has shown that the most significant risk factors causing CRC include lifestyle, diet, and environmental factors, including consumption of red meat, cigarettes, and excessive intake of alcohol (Honari et al., 2019). CRC primarily begins in the bowel lining and can expand throughout the bowel wall if left untreated (Gulbake et al., 2016). Cytotoxic drugs, chemotherapy,

radiotherapy, and surgery are usually the basis for conventional cancer treatment (Aiello et al., 2019). Besides the therapies mentioned above, the use of natural compounds has become a new horizon in the treatment of a wide range of diseases, such as cancer (Honari et al., 2019).

Many studies have revealed that various biologically active compounds possess anticancer or immune modulatory effects (Subramaniam et al., 2019). Andrographolide is a diterpenoid lactone, which is the major bioactive compound present in the plant *Andrographis paniculata* (Brahmachari, 2017). Andrographolide has been reported to possess many pharmacological effects, such as immunomodulatory, anti-inflammatory, and cytotoxic activity (Khan et al., 2018). Studies

* Corresponding authors.

E-mail addresses: priyak08@gmail.com (P. Kannappan), thiyagaramesh@gmail.com (T. Ramesh).

¹ These authors contributed equally to this work.

<https://doi.org/10.1016/j.jksus.2024.103261>

Received 13 March 2024; Received in revised form 13 May 2024; Accepted 14 May 2024

Available online 16 May 2024

1018-3647/© 2024 The Authors. Published by Elsevier B.V. on behalf of King Saud University. This is an open access article under the CC BY license (<http://creativecommons.org/licenses/by/4.0/>).

revealed andrographolide exhibits significant antiproliferative activity on CRC cells by inducing apoptosis through the generation of ROS, leading to the depolarization of the mitochondrial membrane (Khan et al., 2018). The low bioavailability of andrographolide, which is about 2.67 %, is responsible for its poor therapeutic application (Pawar et al., 2016). In order to improve the therapeutic potential of andrographolide, researchers have developed different drug delivery systems.

In pharmaceutical science, the tendency of a dosage form to come into close contact with biological surfaces with the help of attractive interactions termed as bio-adhesion (Shaikh et al., 2011). The biological surface may be either epithelial cells or the mucus layer; if the contact takes place between the mucous layer and the dosage form, then the process is termed muco-adhesion (Brahmbhatt, 2017). Using delivery systems with the property of muco-adhesion can enhance the efficiency of andrographolide (Pawar et al., 2016). The residence time of the dosage form at the target site can be prolonged using a muco-adhesive drug delivery system (Boddupalli et al., 2010). Controlled release of both hydrophilic and hydrophobic drugs for a long time can be achieved by selecting suitable polymers, which play a major role in prolonged release of drugs (Hwang and Shin, 2018). Chitosan is a biopolymer which is positively charged and has a broad range of applications in the field of biochemistry. The cationic nature of chitosan used in drug delivery system aids in muco-adhesion (TM et al., 2018). Adhering to the surface of the cells and crosslinking with multivalent ions is made possible by chitosan using its cationic nature. Retention of the drug for a long period to the target site is achieved by the bio-adhesive property of chitosan (Kumar Mehata et al., 2019). Another polymer, pectin, when used along with chitosan, produces a polymer complex that is stable in nature. Pectin is a negatively charged and water-soluble polymer. The polymer complex retains its stability until the pectin part is degraded by the enzyme pectinase released by the microflora present in the colon (Sabra et al., 2019).

Decorating the surface of nanoparticles with ligands that can bind to the target receptors overexpressed on the cancer cell surface can be used to improve the target specificity of drug-loaded nanoparticles. Nanoparticles are targeted selectively by differentiating the specific kind of biomarkers that are overexpressed on cancer cells but not in normal cells (Kumar Mehata et al., 2019). Vascular Endothelial Growth Factor (VEGF) and Epidermal Growth Factor Receptors (EGFR) are the two major molecular markers and receptors that play a specific role in CRC growth and metastasis (Akbarzadeh Khiavi et al., 2019). Monoclonal antibodies targeting these receptors have been approved recently by the FDA. These monoclonal antibodies are either humanised or chimeric, and they can specifically target the cancer cells and kill them. The monoclonal antibodies that are used in CRC treatment include cetuximab, bevacizumab, and panitumumab (Noguchi et al., 2013).

Cetuximab is a chimeric monoclonal antibody that is designed to prevent EGF from binding to EGFR, which in turn blocks the signal transduction pathway leading to cell cycle arrest, inhibition of progression and metastasis, angiogenesis inhibition, and apoptosis induction (Bou-Assaly and Mukherji, 2010). The study deals with the investigation of the synergetic effect of cetuximab-conjugated bio-adhesive nanoparticles loaded with andrographolide for targeted delivery of andrographolide for CRC therapy against 1,2-dimethylhydrazine (DMH) in mice.

2. Materials and methods

2.1. Preparation of andrographolide loaded chitosan-pectin nanoparticles

Andrographolide loaded chitosan-pectin composite nanoparticles (Ch-Pec-Andro- NPs) was formulated using method by Sabra (Sabra et al., 2019) with slight modification. Briefly, 500 µl of andrographolide solution (10 mg/ml in ethanol) was added dropwise to 10 mL of pectin solution (0.5 mg/ml) dissolved in deionized water, followed by 10 mL of chitosan (2.5 mg/mL) in 2 % v/v acetic acid, which was then adjusted to

pH 5 using 2 M NaOH and 0.5 mg/mL of sodium tripolyphosphate was added to the solution mixture dropwise. The formulation process was carried out for 20 min with 500 rpm in a magnetic stirrer and then stored at 4 °C for further analyses.

2.2. Conjugation of cetuximab to the nanoparticles

The conjugation of cetuximab to the Ch-Pec-Andro-NPs was carried out as described previously (Duwa et al., 2020). In order to activate the carboxyl groups of the nanoparticles, the solution was stirred for 15 min after 2 mg of lyophilized Ch-Pec-AndroNPs were dispersed in 2-Morpholinoethanesulphonic acid (MES) buffer (0.1 M, pH 8.5). Then, 5 mM N-Hydroxysuccinimide (NHS) solution was added. After stirring for 20 min, cetuximab was added, and the process continued for a further 4 h. Followed by the centrifugation at 17,000 rpm for 30 min was used to recover Cet-Ch-Pec-Andro-NPs, which were then twice washed with PBS buffer solution, pH 7.4). The next step was to collect Cet-Ch-Pec-Andro-NPs by centrifugation in order to calculate the Cetuximab conjugation efficiency (CE) and lyophilize them for further research. Without Cetuximab, Ch-Pec-Andro-NPs were created in the same way.

2.3. In-vivo studies

The approved protocols for the biochemical and histopathological analysis were followed during the in vivo tests. All animals were cared for in accordance with the standards outlined in the guide for the care and use of laboratory animals. Male Swiss Albino mice (4–6 weeks old, weighing 20–25 g) were procured from the Kerala veterinary and Animal Sciences University at Thrissur, India. The approval for the animal study were obtained from the Institutional Animal Ethical Committee (494/IAEC/2021) PSG Institute of Medical Science Research, Coimbatore, India. The experiment involved six groups: a control group (Group 1), a group treated with DMH at a dose of 20 mg/kg via the subcutaneous route (Group 2), a group treated with free andrographolide at a dose of 5 mg/kg via the intravenous route (Group 3), a group treated with Ch-Pec-Andro-NPs (equivalent to 5 mg/kg of andrographolide) via the intravenous route (Group 4), a group treated with Cet-Ch-Pec-Andro-NPs (equivalent to 5 mg/kg of andrographolide) via the intravenous route (Group 5), and a group treated with 5-Fluorouracil at a dose of 40 mg/kg via the intraperitoneal route. The andrographolide (5 mg/kg b.wt) was administered based on previously published preclinical studies (Yen et al., 2018).

Following the experimental protocol, the animals were sacrificed while being sedated with ketamine. Heart puncture blood was drawn into centrifuge tubes with and without EDTA, plasma and serum were separated for further biochemical analysis. Liver and the colon tissues were immediately excised, thoroughly washed with ice cold physiological saline, and then dried. For histopathological analysis, a portion of the colon tissues were fixed in 10 % formalin. Liver and colon tissue homogenate were prepared by using a homogenizer and ice-cold potassium chloride.

2.3.1. Body weight analysis and identification of ACF

The body weight of each mouse was assessed using a sensitive balance during the acclimatization period. For the identification of ACF, the colon was separated, flushed with saline, opened from the cecum to the anus, divided into three segments, and fixed flat between two pieces of filter paper in 10 % buffered formalin. The filter paper was covered with microscopic slides to guarantee that the tissue would stay flat during fixation. According to Bird and Good (Bird and Good, 2000), the colon was stained with 0.2 % methylene blue after spending 24 h in buffered formalin. Once again on a microscopic slide, it was placed mucosal side up, and a light microscope was used to observe it.

2.3.2. Haematological profile analysis

The whole blood sample was used for the estimation of

Table 1

Effects of Ch-Pec-Andro-NPs and Cet-Ch-Pec-Andro-NPs on body weight. The data are shown as the mean \pm SD of six mice in each group. Values that do not share a common superscript letter (a-d) differ significantly at $P < 0.05$ (DMRT).

Groups	Body weight (g)	
	Initial	Final
Control	19.7 \pm 0.44	26.95 \pm 0.5 ^a
DMH	19.9 \pm 0.51	19.53 \pm 0.33 ^d
Andro	19.9 \pm 0.84	23.4 \pm 0.24 ^{bc}
NPs	20.2 \pm 0.54	22.93 \pm 0.18 ^c
Ab-NPs	20.5 \pm 0.58	24 \pm 0.19 ^b
5-FU	19.9 \pm 0.47	23.75 \pm 0.42 ^{bc}

haematological parameters such as haemoglobin (Hb), red blood cells (RBC), white blood cells (WBC), packed cell volume (PCV) and platelets and it was performed by using SYSMEX Kx -21(Eraba, Transasia, Kobe-Japan) automatic haematology analyser.

2.3.3. Biochemical parameters

Liver function markers likely aspartate transaminase (AST) and alanine transaminase (ALT), alkaline and acid phosphatase (ALP and ACP) were estimated. Kidney function markers such as protein, albumin,

urea, creatinine, and uric acid were estimated. Antioxidants like catalase (CAT), reduced glutathione (GSH), superoxide dismutase (SOD), glutathione peroxidase (GPx), vitamin-C. Also, the lactate dehydrogenase (LDH) and lipid peroxidase (LPO/MDA) was estimated. While the serum was used to estimate total cholesterol (Erba ® kit), carcinoembryonic antigen (CEA), cancer antigen 125 (CA125), low density lipoproteins (LDL), very low-density lipoproteins (VLDL), high density lipoproteins (HDL), and Triglycerides (TRG).

2.3.4. Histopathological analysis

For the histopathological study, the colonic tissue was excised, preserved in 10 % formalin, and tissue blocks were prepared. Using a 4 times magnification microscope, a thin section of tissue was stained with haematoxylin and eosin stain and were then examined.

2.4. Statistical analysis

Values are presented as mean \pm SD. One-way analysis of variance (ANOVA) and Duncan's Multiple Range Test were used to analyse the difference between the means of the six groups that was statistically significant. Means with a P value < 0.05 , were considered statistically significant. The software suite SPSS 16.0 was used to conduct the statistical analysis (SPSS, IBM product, Chicago, IL, USA).

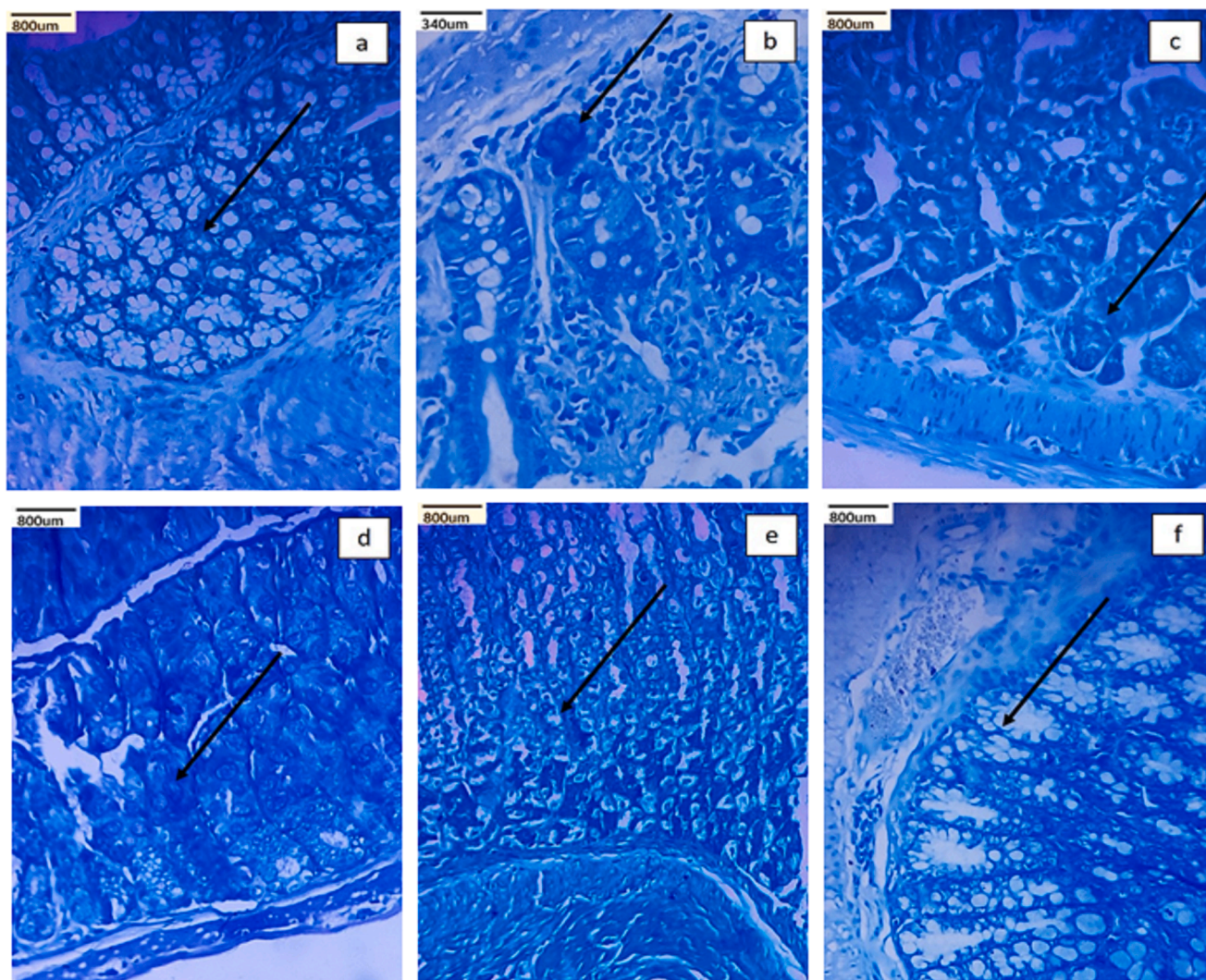


Fig. 1. Identification of crypts with abnormal foci in various treatment groups including a) control, b) DMH treated, c) Andrographolide treated, d) Ch-Pec-Andro-NPs treated, e) Cet-Ch-Pec-Andro-NPs treated, and f) 5-FU groups.

Table 2

Effects of Ch-Pec-Andro-NPs and Cet-Ch-Pec-Andro-NPs on haematological parameters. The data are shown as the mean ± SD of six mice in each group. Values that do not share a common superscript letter (a-d) differ significantly at P < 0.05 (DMRT).

Groups	Hb (g/dl)	PCV (%)	RBC (millions/mm ³)	WBC (Thousands/mm ³)	Platelets (lakhs/mm ³)
Control	13.32 ± 0.12 ^a	40.08 ± 0.34 ^a	4.45 ± 0.1 ^a	8 ± 0.21 ^e	6.5 ± 0.14 ^d
DMH	8.85 ± 0.52 ^d	26.08 ± 1.28 ^d	2.9 ± 0.18 ^e	10.27 ± 0.15 ^a	7.85 ± 0.11 ^a
Andro	9.5 ± 0.14 ^c	28.67 ± 0.47 ^c	3.47 ± 0.08 ^d	9.42 ± 0.15 ^b	6.9 ± 0.18 ^{bc}
Ch-Pec-Andro-NPs	10.42 ± 0.15 ^b	31.07 ± 0.36 ^b	3.58 ± 0.12 ^{cd}	8.57 ± 0.16 ^d	7.06 ± 0.27 ^b
Cet-Ch-Pec-Andro-NPs	10.48 ± 0.12 ^b	31.37 ± 0.48 ^b	3.65 ± 0.14 ^{bc}	8.9 ± 0.24 ^c	6.85 ± 0.10 ^{bc}
5-FU	10.48 ± 0.12 ^b	31.55 ± 0.21 ^b	3.75 ± 0.1 ^b	9.02 ± 0.4 ^c	6.65 ± 0.38 ^{cd}

Table 3

Effects of Ch-Pec-Andro-NPs and Cet-Ch-Pec-Andro-NPs on liver markers. The data are shown as the mean ± SD of six mice in each group. Values that do not share a common superscript letter (a-d) differ significantly at P < 0.05 (DMRT). AST, ALT, LDH – μ moles of pyruvate liberated /L, ALP, ACP – μ moles of phenol liberated /L.

Groups	AST	ALT	ALP	ACP	LDH
Control	37.23 ± 1.19 ^c	33.42 ± 0.62 ^d	78.05 ± 3.21 ^e	5.37 ± 0.16 ^c	253.65 ± 8.48 ^d
DMH	46.9 ± 1.77 ^b	54.03 ± 1.46 ^a	96.03 ± 2.42 ^a	6.17 ± 0.26 ^a	274.9 ± 8.01 ^c
Andro	38.2 ± 1.64 ^c	40.35 ± 3.3 ^b	87.12 ± 1.69 ^c	5.42 ± 0.1 ^c	269.37 ± 5.18 ^c
Ch-Pec-Andro-NPs	34.7 ± 1.47 ^d	37.05 ± 1.68 ^c	81.6 ± 0.91 ^d	5.33 ± 0.08 ^c	269.55 ± 8.42 ^c
Cet-Ch-Pec-Andro-NPs	33.72 ± 1.01 ^d	34.43 ± 1.18 ^d	91.2 ± 4.93 ^b	5.63 ± 0.16 ^b	260.17 ± 7.88 ^d
5-FU	35 ± 1.7 ^d	34.68 ± 0.89 ^d	85.9 ± 1.99 ^c	5.38 ± 0.15 ^c	255.78 ± 3.02 ^d

3. Results

3.1. Body weight and identification of ACF

The results from the present study revealed that the DMH-treated group had lower body weights than the control group. However, the loss of body weight in all the treatment groups were significantly (P < 0.05) prevented among the treated groups Cet-Ch-Pec-Andro-NPs displayed good improvement in body weight. (Table 1). Additionally, mice treated with Cet-Ch-Pec-Andro-NPs and 5FU had significantly less to no ACF and less intense methylene blue than those treated with DMH (Fig. 1b, e, & f). The colons of control mice lacked any crypts that were not regular (Fig. 1a).

3.2. Haematological parameters

Hemoglobin (HB), Red Blood Corpuscles (RBC), and Packed cell volume (PCV) levels (Table 2) was found to be significantly decreased in DMH-treated group than the control group, whose levels has been found to be improved in the Andro, Ch-Pec-Andro-NPs, and Cet-Ch-Pec-Andro-NPs treated groups. Significantly elevated levels of platelets and White Blood

Table 4

Effects of Ch-Pec-Andro-NPs and Cet-Ch-Pec-Andro-NPs on renal markers. The data are shown as the mean ± SD of six mice in each group. Values that do not share a common superscript letter (a-d) differ significantly at P < 0.05 (DMRT).

Groups	Urea (mg/dl)	Creatinine (mg/dl)	UA (mg/dl)	T. Protein (g/dl)	Albumin (g/dl)
Control	27.62 ± 1.18 ^b	0.5 ± 0.05 ^a	1.58 ± 0.24 ^b	6.58 ± 0.15 ^a	3.6 ± 0.14 ^a
DMH	32.12 ± 2.47 ^a	0.46 ± 0.01 ^{ab}	2.53 ± 0.12 ^a	5.07 ± 0.18 ^c	3.07 ± 0.22 ^c
Andro	26.88 ± 1.3 ^b	0.48 ± 0.02 ^a	1.38 ± 0.12 ^c	6.1 ± 0.24 ^b	3.27 ± 0.16 ^b
Ch-Pec-Andro-NPs	23.57 ± 0.85 ^c	0.47 ± 0.04 ^{ab}	1.33 ± 0.12 ^c	6.57 ± 0.16 ^a	3.55 ± 0.1 ^a
Cet-Ch-Pec-Andro-NPs	30.4 ± 2.29 ^a	0.49 ± 0.03 ^a	1.37 ± 0.1 ^c	6.37 ± 0.16 ^a	3.43 ± 0.16 ^{ab}
5-FU	29.93 ± 2.31 ^a	0.44 ± 0.01 ^b	1.4 ± 0.14 ^c	6.43 ± 0.16 ^a	3.33 ± 0.12 ^b

Table 5

Effects of Ch-Pec-Andro-NPs and Cet-Ch-Pec-Andro-NPs on the antioxidant enzymes and lipid peroxidation. The data are shown as the mean ± SD of six mice in each group. Values that do not share a common superscript letter (a-d) differ significantly at P < 0.05 (DMRT).

Groups	SOD	CAT	GPX	GSH	VIT C	LPO
Control	7.42 ± 0.31 ^a	44.48 ± 1.24 ^a	8.5 ± 0.14 ^a	55.23 ± 2 ^a	4.5 ± 0.14 ^a	24.27 ± 1.39 ^d
DMH	4.7 ± 0.17 ^e	30.42 ± 1.49 ^d	7.27 ± 0.4 ^d	24.43 ± 1.71 ^d	3.33 ± 0.16 ^c	78.32 ± 4.36 ^a
Andro	6.68 ± 0.12 ^{bc}	38.12 ± 1.04 ^c	7.38 ± 0.21 ^d	36.83 ± 1.52 ^c	4.27 ± 0.16 ^b	52.43 ± 4.34 ^c
Ch-Pec-Andro-NPs	6.37 ± 0.16 ^d	43.85 ± 1.51 ^a	7.73 ± 0.38 ^c	39.93 ± 2.71 ^{bc}	4.3 ± 0.14 ^b	54.28 ± 1.12 ^{bc}
Cet-Ch-Pec-Andro-NPs	6.55 ± 0.19 ^{cd}	43.6 ± 0.89 ^a	8.33 ± 0.12 ^{ab}	40.08 ± 4.57 ^{bc}	4.58 ± 0.17 ^a	56.97 ± 1.58 ^b
5-FU	6.9 ± 0.18 ^b	40.3 ± 1.65 ^b	8.03 ± 0.31 ^b	41.97 ± 2.24 ^b	4.58 ± 0.15 ^a	57.33 ± 1.22 ^b

Corpuscles (WBC) were observed in the DMH-treated group than the control group. In the Andro, Ch-Pec-Andro-NPs, and Cet-Ch-Pec-Andro-NPs treated groups platelets and WBC levels were reverted to normal level.

3.3. Liver and renal function markers

In this study, the DMH-treated group had higher levels of ALP and ACP than the control group, and significantly decreased levels of AST and ALT in the DMH treated group when compared to the control group. Among the treatment group Cet-Ch-Pec-Andro-NPs-treated group was found to have the levels of ALP, ACP, AST, and ALT similar to that of the control group (Table 3). Decreased levels of urea, creatinine, total protein, and albumin and elevated uric acid levels were observed in the DMH-treated group. Urea and creatinine levels were improved in the Cet-Ch-Pec-Andro-NPs treated group (Table 4).

3.4. Antioxidant enzymes and lipid peroxidation

The significant decrease in the level of antioxidant enzymes such as SOD, CAT, GPx, GSH and Vit C in the DMH-treated groups was found to be reverted back to the normal level in the treatment groups (Table 5). Results showed that the significantly elevated level of lipid peroxidation in the DMH-treated group and was found to be reduced in the treatment groups.

Table 6

Effects of Ch-Pec-Andro-NPs and Cet-Ch-Pec-Andro-NPs on the lipid profile. The data are shown as the mean \pm SD of six mice in each group. Values that do not share a common superscript letter (a-d) differ significantly at $P < 0.05$ (DMRT).

Groups	T. Cho (mg/dl)	TGL (mg/dl)	HDL (mg/dl)	LDL (mg/dl)	VLDL (mg/dl)
Control	90.52 \pm 2.01 ^{ab}	75.14 \pm 2.36 ^c	53.92 \pm 1.26 ^a	61.45 \pm 1.76 ^f	16.68 \pm 0.96 ^{cd}
DMH	87.1 \pm 0.32 ^{cd}	94.12 \pm 0.71 ^a	24.3 \pm 1.61 ^d	97.78 \pm 3.61 ^a	38.75 \pm 3.12 ^a
Andro	91.35 \pm 6.16 ^{bc}	81.98 \pm 2.72 ^b	36.23 \pm 2.23 ^c	85.83 \pm 0.67 ^b	25.5 \pm 2.64 ^b
Ch-Pec-Andro-NPs	84.68 \pm 1.55 ^d	74.13 \pm 1.15 ^c	46.85 \pm 1.7 ^b	81.73 \pm 1.25 ^c	18.83 \pm 1.47 ^c
Cet-Ch-Pec-Andro-NPs	91.96 \pm 2.82 ^a	71.83 \pm 0.76 ^d	46.27 \pm 1.89 ^b	75.48 \pm 0.71 ^d	17.17 \pm 1.55 ^{cd}
5-FU	87.75 \pm 3.77 ^{bc}	75.45 \pm 1.94 ^c	46.5 \pm 0.71 ^b	72.27 \pm 2.51 ^e	15.9 \pm 0.43 ^d

3.5. Lipid profile

Among the lipids TRG, LDL, and VLDL were significantly increased in the DMH-treated group than the control group. The elevated levels of the above-mentioned lipids were found to be gradually decreased in the treatment group. In the Cet-Ch-Pec-Andro-NPs treated group the level of these levels was reverted to the control group. Significant decrease in the levels of HDL was observed in the DMH-treated group than the control group. While the decrease in the total cholesterol levels were not significant. Increase in the level of HDL was noticed in the treatment groups (Table 6).

3.6. Serum CRC markers

In the DMH-treated group sharp rise in the levels of the serum CEA and CA 125 were observed than the control group. A significant decrease in the levels of CEA and CA125 was observed in the treatment group among which 5-FU and Cet-Ch-Pec-Andro-NPs treated groups demonstrated the optimum decline in the levels of the above-mentioned serum CRC markers (Table 7).

3.7. Histopathological examination

Histopathological examination revealed that the control group tissue retained their typical tissue architecture and crypt morphology (Fig. 2a). On the other hand, the colonic cells in the DMH-treated groups (Fig. 2b) showed clear histological abnormalities, such as distorted crypts, increased inflammatory infiltrates, crypt distortion, and mucosal sloughing, which indicated cancerous transformation. In groups treated with andrographolide, there were mild inflammatory infiltrates and cryptitis (Fig. 2c). Only a few inflammatory infiltrates, a normal muscular layer, and crypts were visible in the Ch-Pec-Andro-NPs treated groups (Fig. 2d). Treatment with Cet-Ch-Pec-Andro-NPs and 5-fluorouracil resulted in the regeneration of crypts, a normal muscular layer, an increase in the number of normal crypts, and a decrease in inflammatory infiltrates (Fig. 2e & f).

4. Discussion

Globally, CRC is a leading cause of death. The frequent recurrence of CRC and the emergence of a drug-resistant form of the disease are indicators of the efficacy of the current treatment protocols (De et al., 2023). Recent epidemiologic findings have emphasised the link between consuming a number of foods and nutrients that are high in phytochemicals and a reduced risk of CRC. Preclinical studies show that dietary phytochemicals regulate various markers and signalling pathways to have chemopreventive effects on CRC cells (Afrin et al., 2020). Andrographolide, a phytomolecule from *Andrographis paniculata*,

Table 7

Effects of Ch-Pec-Andro-NPs and Cet-Ch-Pec-Andro-NPs on colorectal cancer serum markers. The data are shown as the mean \pm SD of six mice in each group. Values that do not share a common superscript letter (a-d) differ significantly at $P < 0.05$ (DMRT).

Groups	CEA (ng/dl)	CA 125 (ng/dl)
Control	0.45 \pm 0.05 ^e	0.52 \pm 0.08 ^d
DMH	3.95 \pm 0.43 ^a	2.45 \pm 0.1 ^a
Andro	2.72 \pm 0.21 ^b	1.32 \pm 0.1 ^c
Ch-Pec-Andro-NPs	2.07 \pm 0.39 ^c	1.38 \pm 0.12 ^c
Cet-Ch-Pec-Andro-NPs	1.62 \pm 0.12 ^c	1.18 \pm 0.28 ^c
5-FU	1.38 \pm 0.12 ^d	1.88 \pm 0.23 ^b

combats all signalling molecules and pathways that support tumour growth (Paul et al., 2021). Combining phytochemicals with targeted therapy is a highly effective way to treat CRC.

Carcinogen-induced tumour models would be interesting to study the effectiveness of immunotherapeutic agents because tumour immunogenicity plays a key role in predicting the response to immunotherapies (Guerin et al., 2020). The most frequently used chemical to induce CRC in animal models is 1,2-dimethylhydrazine (DMH). Colorectal tumours caused by DMH, a powerful colon carcinogen, resemble human colorectal cancer in many ways, including how they react to some promoters and preventative medications (El-Khadragy et al., 2018).

CRC and weight loss are linked, and the primary factor that could be causing the weight loss is the colon epithelium's decreased function, which was primarily brought on by a widespread inflammation that reduced feed absorption (Reis et al., 2022). In a similar study administration of n-butylenephthalide to the DMH-treated disease control improved the weight loss caused due to CRC (Bantal et al., 2016). Inflammation is a fundamental factor in tumorigenesis and growth. Local and systemic inflammatory responses promote a microenvironment that supports the growth of cancer cells. Numerous retrospective studies agree that haematological parameters reflect the balance of inflammatory responses and immune system function. In the present study, the significant changes in the hematological parameters observed in the DMH-treated group were improved in the treatment groups, which may be due to the immune stimulatory (Vetvicka and Vannucci, 2021) and improved hemopoiesis activity of andrographolide (Rajendrakumar et al., 2020). ACF is typically regarded as the earliest detectable macroscopic lesion in the colonic mucosa that may be associated with a risk of developing a neoplasm eventually (Drew et al., 2013). Given this information, we examined the colonic ACFs using methylene blue staining to confirm the induction of CRC.

Numerous tissue marker enzymes, such as ACP, ALP, ALT, and AST, appear to become more active after any injury to the liver or hepatic tissues. Serum liver enzyme levels were significantly different in the DMH-treated group, indicating the hepatic injury caused by DMH during carcinogenesis. The hepatoprotective properties of andrographolide (Trivedi et al., 2007) may be essential for preserving serum liver markers and liver health, which will increase survival rates for people with CRC. The systemic inflammatory state of the patient, the decrease in water intake due to loss of appetite, and diarrhoea brought on by changes in the intestinal environment have all been linked to damage to renal function during CRC (Yang et al., 2021). The changes in the serum renal markers due to CRC were controlled in the treatment groups.

Lipids may also be involved in how cancer cells adapt, in addition to the change in glucose and glutamine metabolism. It is common knowledge that cancer cells exhibit changes in lipid metabolism (Huang and Freter, 2015). Synthesis, elongation, desaturation, and mitochondrial oxidation of fatty acids are among the lipid metabolic pathways affected in CRC cells (Sung et al., 2021). In the present study, abnormal levels of lipids were restored in the treatment groups. The decrease in lipid levels may be contributed by the hypolipidemic activity of andrographolide (Rajaratnam and Nafi, 2019).

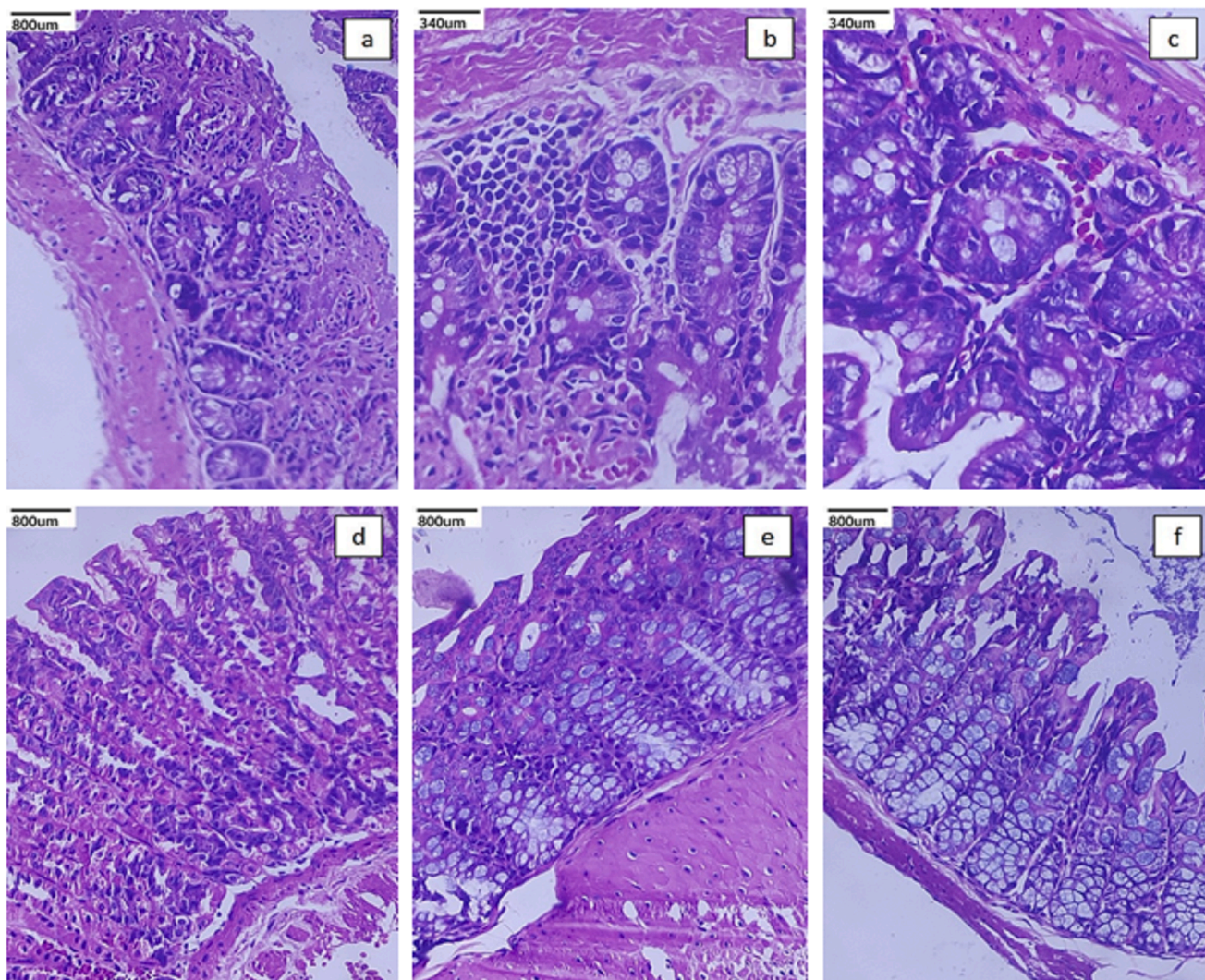


Fig. 2. Colon tissue histopathological depiction (a). The control group exhibits crypts and muscle layer that appear normal (b). In contrast, the DMH treated group displays mucosal sloughing and surface disintegration (c). The group treated with andrographolide (d), the group treated with Ch-Pec-Andro-NPs (e), the group treated with Cet-Ch-Pec-Andro-NPs (f), and the group treated with 5-FU all exhibited a normal muscle layer and regenerated crypts.

The level of antioxidant defence and lipid peroxidation have both been suggested as helpful indicators for estimating the likelihood of oxidative damage-induced carcinogenesis (Muthu et al., 2013). Free radicals are neutralised by the natural antioxidants SOD, CAT, GPx, GR, and GSH, which also shield cells from oxidative stress. The main endogenous antioxidants, SOD and CAT, directly destroy free radicals, while GPx detoxifies H₂O₂, making these enzymes important in the fight against ROS. Innate antioxidant defence mechanisms are activated by non-protein thiol, GSH, and dependent enzymes. It's possible that tumour cells' increased use of tissue antioxidants in the detoxification of harmful DMH metabolites is what caused the tissue antioxidant levels to decline in DMH-exposed mice. While in the treatment groups, antioxidant levels were restored, allowing them to use their scavenging mechanisms to inhibit the growth of colorectal tumours, indicating that andrographolide protects cells from DMH-induced neoplastic transformation.

High levels of CEA are present in 70 % of CRC patients at the time of diagnosis, making it an excellent marker for disease treatment and surveillance following resection (Jelski and Mroczko, 2020). Owing to the highly heterogeneous character of CRC, it is doubtful that a single tumour marker will serve as a reliable diagnostic criterion with enough sensitivity or specificity for all instances. As additional markers for CRC

diagnosis, postoperative surveillance, and the observation of therapeutic benefits, CA19-9, CA125, and CA242 have been employed (Luo et al., 2020). A decline in the levels of CEA and CA-125 in the treatment groups indicates a positive prognosis and the ability of andrographolide to prevent neoplastic growth.

5. Conclusion

The present study shows that anti-EGFR antibody-surface-modified chitosan-pectin composite nanoparticles efficiently load the phyto-compound andrographolide, enhancing its chemotherapeutic effects in DMH-treated mice. Comparatively to andrographolide (Andro) and andrographolide-loaded chitosan pectin composite nanoparticles, cetuximab-conjugated andrographolide-loaded chitosan pectin nanoparticles (Cet-Ch-Pec-Andro-NPs) restored the abnormal levels of the majority of serum and colon markers caused by the DMH treatment (Ch-Pec-Andro-NPs). The improved anticancer activity of the conjugated nanoparticles must be due to the targeted delivery of andrographolide to the cancer cells made possible by the conjugation of the EGFR antibody. Even though Cet-Ch-Pec-Andro-NPs showed improved anticancer activity, increasing the concentration of EGFR antibodies can increase the therapeutic potency of these nanoparticles. Therefore, our results

suggest that Cet-Ch-Pec-Andro-NPs provide a flexible nanoplatform for drug delivery for the treatment of CRC.

CRedit authorship contribution statement

Janani Balakarthikeyan: Writing – original draft, Visualization, Investigation. **Vijayakumar Mayakrishnan:** Writing – review & editing, Writing – original draft, Visualization, Software, Methodology, Investigation, Conceptualization. **Priya Kannappan:** Writing – review & editing, Writing – original draft, Visualization, Software, Methodology, Investigation, Conceptualization. **Sameer Al-Ghamdi:** Writing – review & editing, Visualization, Supervision, Methodology, Investigation, Conceptualization. **Naif Abdurhman Alrudian:** Writing – review & editing, Visualization, Supervision, Software, Methodology, Investigation, Conceptualization. **Mohammed Saad Alqahtani:** Writing – original draft, Visualization, Investigation, Data curation. **Mahmoud H. El-Bidawy:** Writing – original draft, Visualization, Investigation, Data curation. **Khalid Albasheer:** Writing – review & editing, Validation, Software. **Sahar Gamil:** Writing – original draft, Visualization, Investigation, Data curation. **Nesreen Alsanousi:** Writing – review & editing, Validation, Software. **Thiyagarajan Ramesh:** Writing – review & editing, Validation, Software.

Declaration of competing interest

The authors declare that they have no known competing financial interests or personal relationships that could have appeared to influence the work reported in this paper.

Acknowledgements

The authors are grateful to the Deanship of Scientific Research, Prince Sattam Bin Abdulaziz University, Al-Kharj, Saudi Arabia for its support for this research work.

Appendix A. Supplementary data

Supplementary data to this article can be found online at <https://doi.org/10.1016/j.jksus.2024.103261>.

References

- Afrin, S., Giampieri, F., Gasparrini, M., et al., 2020. Dietary phytochemicals in colorectal cancer prevention and treatment: a focus on the molecular mechanisms involved. *Biotechnol. Adv.* 38, 107322 <https://doi.org/10.1016/j.biotechadv.2018.11.011>.
- Aiello, P., Sharghi, M., Mansourkhani, S.M., et al., 2019. Medicinal plants in the prevention and treatment of colon cancer. *Oxid. Med. Cell. Longev.* 2019, 2075614. <https://doi.org/10.1155/2019/2075614>.
- Akbarzadeh Khiavi, M., Safary, A., Somi, M.H., 2019. Recent advances in targeted therapy of colorectal cancer: impacts of monoclonal antibodies nanoconjugates. *Bioimpacts* 9 (3), 123–127. <https://doi.org/10.15171/bi.2019.16>.
- Bantal, V., Baseeruddin Alvi, S., Archana, K., 2016. Protective effect of n-butylideneephthalide against 1, 2-dimethylhydrazine induced colon cancer in mice. *Pharmacologia* 7, 150–156. <https://doi.org/10.5567/pharmacologia.2016.150.156>.
- Bird, R.P., Good, C.K., 2000. The significance of aberrant crypt foci in understanding the pathogenesis of colon cancer. *Toxicol. Lett.* 112–113, 395–402. [https://doi.org/10.1016/S0378-4274\(99\)00261-1](https://doi.org/10.1016/S0378-4274(99)00261-1).
- Boddupalli, B.M., Mohammed, Z.N., Nath, R.A., et al., 2010. Mucoadhesive drug delivery system: an overview. *J. Adv. Pharm. Technol. Res.* 1 (4), 381–387. <https://doi.org/10.4103/0110-5558.76436>.
- Bou-Assaly, W., Mukherji, S., 2010. Cetuximab (erbitux). *AJNR Am. J. Neuroradiol.* 31 (4), 626–627. <https://doi.org/10.3174/ajnr.A2054>.
- Brahmachari, G., 2017. Andrographolide: A Molecule of Antidiabetic Promise, pp. 1–27. *Brahmbhatt, D., 2017. Bioadhesive drug delivery systems: Overview and recent advances. Int. J. Chem. Life Sci.* 6, 2016. <https://doi.org/10.21746/ijcls.2017.3.1>.
- De, S., S. Paul, A. Manna, et al., 2023. Phenolic Phytochemicals for Prevention and Treatment of Colorectal Cancer: A Critical Evaluation of In Vivo Studies. *Cancers (Basel)*. 15 (3) Doi: [10.3390/cancers15030993](https://doi.org/10.3390/cancers15030993).
- Drew, D.A., Devers, T., Horelik, N., et al., 2013. Nanoproteomic analysis of extracellular receptor kinase-1/2 post-translational activation in microdissected human hyperplastic colon lesions. *Proteomics* 13 (9), 1428–1436. <https://doi.org/10.1002/pmic.201200430>.

- Duwa, R., A. Banstola, F. Emami, et al., 2020. Cetuximab conjugated temozolomide-loaded poly (lactic-co-glycolic acid) nanoparticles for targeted nanomedicine in EGFR overexpressing cancer cells. *J. Drug Deliv. Sci. Technol.* 60, 101928. Doi: [10.1016/j.jddst.2020.101928](https://doi.org/10.1016/j.jddst.2020.101928).
- El-Khadragy, M.F., Nabil, H.M., Hassan, B.N., et al., 2018. Bone marrow cell therapy on 1,2-dimethylhydrazine (DMH)-induced colon cancer in rats. *Cell. Physiol. Biochem.* 45 (3), 1072–1083. <https://doi.org/10.1159/000487349>.
- Guerin, M.V., Finisguerra, V., Van den Eynde, B.J., et al., 2020. Preclinical murine tumor models: a structural and functional perspective. *Elife* 9. <https://doi.org/10.7554/eLife.50740>.
- Gulbake, A., Jain, A., Jain, A., et al., 2016. Insight to drug delivery aspects for colorectal cancer. *World J. Gastroenterol.* 22 (2), 582–599. <https://doi.org/10.3748/wjg.v22.i2.582>.
- Honari, M., Shafabakhsh, R., Reiter, R.J., et al., 2019. Resveratrol is a promising agent for colorectal cancer prevention and treatment: focus on molecular mechanisms. *Cancer Cell Int.* 19, 180. <https://doi.org/10.1186/s12935-019-0906-y>.
- Huang, C., Freter, C., 2015. Lipid metabolism, apoptosis and cancer therapy. *Int. J. Mol. Sci.* 16 (1), 924–949. <https://doi.org/10.3390/ijms16010924>.
- Hwang, S.W., Shin, J.S., 2018. Pectin-coated curcumin-chitosan microparticles crosslinked with Mg²⁺ for delayed drug release in the digestive system. *Int. J. Polym. Sci.* 2018, 2071071. <https://doi.org/10.1155/2018/2071071>.
- Jelski, W., Mroczko, B., 2020. Biochemical markers of colorectal cancer - present and future. *Cancer Manag. Res.* 12, 4789–4797. <https://doi.org/10.2147/cmar.S253369>.
- Khan, I., Khan, F., Farooqui, A., et al., 2018. Andrographolide exhibits anticancer potential against human colon cancer cells by inducing cell cycle arrest and programmed cell death via augmentation of intracellular reactive oxygen species level. *Nutr. Cancer* 70 (5), 787–803. <https://doi.org/10.1080/01635581.2018.1470649>.
- Kumar Mehata, A., Bharti, S., Singh, P., et al., 2019. Trastuzumab decorated TPGS-chitosan nanoparticles for targeted breast cancer therapy. *Colloids Surf. B Biointerfaces* 173, 366–377. <https://doi.org/10.1016/j.colsurfb.2018.10.007>.
- Muthu, R., Thangavel, P., Selvaraj, N., et al., 2013. Synergistic and individual effects of umbelliferone with 5-fluorouracil on the status of lipid peroxidation and antioxidant defense against 1, 2-dimethylhydrazine induced rat colon carcinogenesis. *Biomedicine & Preventive Nutrition.* 3(1), 74–82. Doi: [10.1016/j.bionut.2012.10.011](https://doi.org/10.1016/j.bionut.2012.10.011).
- Noguchi, T., Ritter, G., Nishikawa, H., 2013. Antibody-based therapy in colorectal cancer. *Immunotherapy* 5 (5), 533–545. <https://doi.org/10.2217/imt.13.35>.
- Paul, S., Roy, D., Pati, S., et al., 2021. The adroitness of andrographolide as a natural weapon against colorectal cancer. *Front. Pharmacol.* 12, 731492. <https://doi.org/10.3389/fphar.2021.731492>.
- Pawar, A., Rajalakshmi, S., Mehta, P., et al., 2016. Strategies for formulation development of andrographolide. *RSC Adv.* 6 (73), 69282–69300. <https://doi.org/10.1039/C6RA12161F>.
- Rajaratnam, H., Nafi, S.N.M., 2019. Andrographolide is an alternative treatment to overcome resistance in ER-positive breast cancer via cholesterol biosynthesis pathway. *Malays J. Med. Sci.* 26 (5), 6–20. <https://doi.org/10.21315/mjms2019.26.5.2>.
- Rajendrakumar, T., Rao, S., Satyanarayana, M., et al., 2020. Hematological alterations in cisplatin induced toxicity in rats and its amelioration by Andrographis paniculata. *Int. J. Curr. Microbiol. App. Sci.* 9, 525–532. <https://doi.org/10.20546/ijemas.2020.904.063>.
- Reis, S.K., Socca, E.A.R., de Souza, B.R., et al., 2022. Effects of combined OncoTherapy immunotherapy and probiotic supplementation on modulating the chronic inflammatory process in colorectal carcinogenesis. *Tissue Cell* 75, 101747. <https://doi.org/10.1016/j.tice.2022.101747>.
- Sabra, R., Billa, N., Roberts, C.J., 2019. Cetuximab-conjugated chitosan-pectinate (modified) composite nanoparticles for targeting colon cancer. *Int. J. Pharm.* 572, 118775. <https://doi.org/10.1016/j.ijpharm.2019.118775>.
- Shaikh, R., Raj Singh, T.R., Garland, M.J., et al., 2011. Mucoadhesive drug delivery systems. *J Pharm Bioallied Sci.* 3 (1), 89–100. <https://doi.org/10.4103/0975-7406.76478>.
- Subramaniam, S., Selvaduray, K.R., Radhakrishnan, A.K., 2019. Bioactive compounds: natural defense against cancer? *Biomolecules* 9 (12). <https://doi.org/10.3390/biom9120758>.
- Sung, H., Ferlay, J., Siegel, R.L., et al., 2021. Global cancer statistics 2020: GLOBOCAN estimates of incidence and mortality worldwide for 36 cancers in 185 countries. *CA Cancer J. Clin.* 71 (3), 209–249. <https://doi.org/10.3322/caac.21660>.
- TM, M. W., W. M. Lau and V. V. Khutoryanskiy, 2018. Chitosan and Its Derivatives for Application in Mucoadhesive Drug Delivery Systems. *Polymers (Basel)*. 10(3) Doi: [10.3390/polym10030267](https://doi.org/10.3390/polym10030267).
- Trivedi, N.P., Rawal, U.M., Patel, B.P., 2007. Hepatoprotective effect of andrographolide against hexachlorocyclohexane-induced oxidative injury. *Integr. Cancer Ther.* 6 (3), 271–280. <https://doi.org/10.1177/1534735407305985>.
- Vetvicka, V., Vannucci, L., 2021. Biological properties of andrographolide, an active ingredient of Andrographis Paniculata: a narrative review. *Ann. Transl. Med.* 9 (14), 1186. <https://doi.org/10.21037/atm-20-7830>.
- Yang, M., Zhang, Q., Ruan, G.T., et al., 2021. Association between serum creatinine concentrations and overall survival in patients with colorectal cancer: a multi-center cohort study. *Front. Oncol.* 11, 710423. <https://doi.org/10.3389/fonc.2021.710423>.
- Yen, C.C., Chen, Y.C., Wu, M.T., et al., 2018. Nanoemulsion as a strategy for improving the oral bioavailability and anti-inflammatory activity of andrographolide. *Int. J. Nanomed.* 13, 669–680. <https://doi.org/10.2147/ijn.S154824>.